# Three-Dimensional (3D) Visualisation of the Cardiovascular System of Mouse Embryos and Fetus

Wolfgang J. Weninger[*] and Stefan H. Geyer

*IMG, Centre for Anatomy and Cell Biology, Medical University of Vienna, Waehringer Str. 13, A-1090, Vienna, Austria*

**Abstract:** The mouse is the most appropriate biomedical model organism for researching the mechanistic function of genetic factors in normal embryogenesis and in the genesis of cardiovascular malformations. Three-dimensional (3D) visualisation of the developing organs of wild type and genetically modified mouse embryos is essential for such research. This paper aims at discussing imaging methods that permit the generation of digital volume data sets, which fit for the virtual 3D visualisation and 3D analysis of the cardiovascular system of mouse embryos and mouse fetus. To cover the spectrum of imaging methods comprehensively, we will start with a short overview about early 3D-reconstruction techniques. This will be followed by a brief discussion why *in vivo* imaging techniques, such as ultrasound (US) or optical coherence tomography (OCT) do not fit for constructing volume data sets that permit virtual 3D visualisation of the cardiovascular system of mouse embryos/fetus. We will then briefly introduce techniques, which permit 3D analysis of the cardiovascular system but do not fit for creating digital volume data (corrosion casts, scanning electron microscopy). Finally, we will focus on describing the advantages and disadvantages, the spectrum of application and the limitations of important modern digital volume data generation methods, such as micro-computed tomography (µCT), micro-magnetic resonance imaging (µMRI), optical projection tomography (OPT), confocal microscopy, histological section based volume data generation methods, and 3D episcopic imaging methods.

## INTRODUCTION

### Scientific Background

Approximately 0.4 - 1% of all live-born humans suffer from congenital heart diseases [1]. Detailed knowledge of the function and the interactions of genetic and epigenetic factors driving normal and abnormal embryogenesis is essential for understanding their aetiology. It will be the key for developing new diagnostic and therapeutic strategies.

### The Mouse as an Important Biomedical Model Organism

Model organisms, such as the mouse, the chick, the frog, and the zebrafish are employed for researching the influence of genetic and epigenetic factors on embryo development. For two reasons, the most important of those models is the mouse. Firstly, the morphology, especially of the cardiovascular system is similar between men and mice. Mice have a four chambered heart with a fully separated outflow tract, parallel pulmonary and systemic circulations, and a left sided aortic arch, which gives rise to three large arteries before - in the prenatal period - it joins with a single ductus arteriosus. Secondly, many sophisticated genetic and transgenic techniques are available to manipulate the mouse genome. This results in transgenic mice carrying reporter genes, or mutants, which show morphological defects.

Targeted gene disruption [2] is one of the techniques, which permits the production of mice with morphological defects. Gene or gene product silencing [3, 4] is another.

Thorough phenotype analysis of the malformed mice provide insights into the function of individual genes and their role in morphogenesis and remodelling of tissues and organs. Another method that alters the mouse genome producing malformations is to feed mutagens to adult mice. The mutagens can randomly introduce point mutations in the germ cells and cause malformations in the offspring. This technique is used to identify new mouse models for human hereditary disorders in the scope of large-scale mutagenesis studies [5, 6].

### Why Imaging Mouse Embryos and Fetus

Obviously the essential first step in characterising a randomly produced or targeted engineered mouse mutant is the careful description of its morphological phenotype. This might be followed by analysing the function of genes with the aid of micro-array techniques [7-12] or by analysing the expression patterns of selected (trans-)genes and gene products in the context of tissue architecture and gross anatomy.

A functioning cardiovascular system is essential for normal organogenesis and *intra-uterine* growth. Therefore cardiovascular malformations are often responsible for prenatal death. Consequently genetically engineered mice, which lack the function of genes involved in cardiovascular morphogenesis must be morphologically analysed as embryos or fetus. Due to the small size of mouse embryos/fetus and due to the lack of sound reference data for qualitative and quantitative analysis, this is a major challenge.

This paper aims at briefly describing methods that permit three-dimensional (3D) visualisation and 3D analyses of the morphology of the cardiovascular system of mouse embryos and fetus. It will discuss their strengths and weaknesses as

*Address correspondence to this author at the IMG, Centre for Anatomy and Cell Biology, Medical University of Vienna, Waehringer Str. 13, A-1090, Vienna, Austria; Tel: ++43-1-4277-61136; Fax: ++43-1-4277-61118; E-mail: Wolfgang.Weninger@meduniwien.ac.at

well as their potency to visualise gene expression patterns in the context of embryo anatomy.

Using strict biological definitions, the prenatal life of all mammals, including rodents, like the mouse, is parted in an embryonic and a fetal period. In mice, the embryonic period lasts from conception to developmental stage 22 according to Theiler [13]. This is approximately embryonic day 14. The fetal period starts with Theiler stage 23 and ends with birth. However, the majority of modern biomedical scientists do not distinguish between mouse embryos and fetus. Instead they use the term embryo for unborn mice of all developmental stages. In the following chapters, we will distinguish between embryos and fetus.

### History of 3D Imaging

Due to the small size of embryos and fetus, their morphology is traditionally analysed with the aid of histological serial sections. But embryos are highly complex three-dimensional (3D) biological objects, and this approach is purely two-dimensional (2D). Therefore the first attempts to create 3D models of embryos and their organs on the basis of histological serial sections date back to the 19th century [14-17].

The early 3D reconstruction methods utilised histologically processed and wax embedded embryos. As in traditional histology, the wax blocks were mounted on microtomes and histological section series were created. The sections were then carefully examined under a microscope. But in contrast to traditional histology, wax, wood, or - in the second part of the 20th century - plexiglas sheets were carved according to the appearance of the microscopic image of every single section. The sheets, which represented subsequent histological sections of a serially sectioned embryo were then stacked together to construct a physical 3D representation of the sectioned embryo (Fig. **1**). Naturally these early 3D reconstruction methods were subjectively biased, error prone and immensely time expensive.

A major breakthrough in terms of feasibility of 3D reconstructions came with the introduction of computers into biomedical research. It was no longer necessary to represent histological sections by plates of wax or other materials or to model solid 3D representations of embryos. Digital images of histological sections could be directly captured with the aid of digital cameras or by scanning micro-photographs taken from sections viewed with a microscope [18, 19]. A number of software packages were developed and allowed processing of these digital images and/or the subsequent generation and visualisation of virtual 3D models [20-22]. These early computer supported 3D reconstruction and visualisation methods essentially followed the same workflow as most modern destructive *post mortem* 3D imaging techniques (see below) and suffered from similar problems.

### Modern 3D Imaging

In the last two decades a number of innovative new 2D and 3D imaging techniques were invented. They are either optimised for diagnosing pathologies in humans (computed tomography (CT), magnetic resonance imaging (MRI), ultrasound (US), single photon emission computed tomography (SPECT), positron emission tomography (PET)), for *in vivo* analysis of – often transparent - model animals [23-32], or

for *post-mortem* analyses of entire biological specimens and biological tissue samples, on the molecular, subcellular, cellular, tissue, and organ system level (atomic force microscopy, electron microscopy, confocal imaging, optical projection tomography (OPT), episcopic imaging techniques, histological sectioning, micro-MRI, micro-CT, near infrared imaging techniques, polarised light spectroscopy, optical coherence tomography (OCT)). Not all of these techniques permit 3D imaging of the developing cardiovascular system of unborn mice. Our study aims at introducing the most promising ones.



**Fig. (1).** Solid three-dimensional (3D) wax model of an embryo. This model is in possession of the Medical University of Vienna.

Most of the modern imaging techniques produce series of digital 2D images. These images can be stacked together to form a digital volume data set, which is the basis for 3D analysis and the generation of virtual 3D models (Fig. **2**).

A digital volume data set is composed of voxels (volume elements). A voxel represents a cube or cuboid, the size of which is best defined by the length of its edges (X x Y x Z) or by its volume. If volume data sets are reconstructed from stacks of subsequent 2D images, the lengths of X and Y are

**Data generation**
(in vivo / post mortem imaging techniques)

↓

**(2D-section images)**
Unit: Pixel

↓

Volume data set from 2D images or directly (CT)
Unit: Voxel

↓

data processing

↓

3D-modelling, 3D-visualisation & 3D-analysis

↓

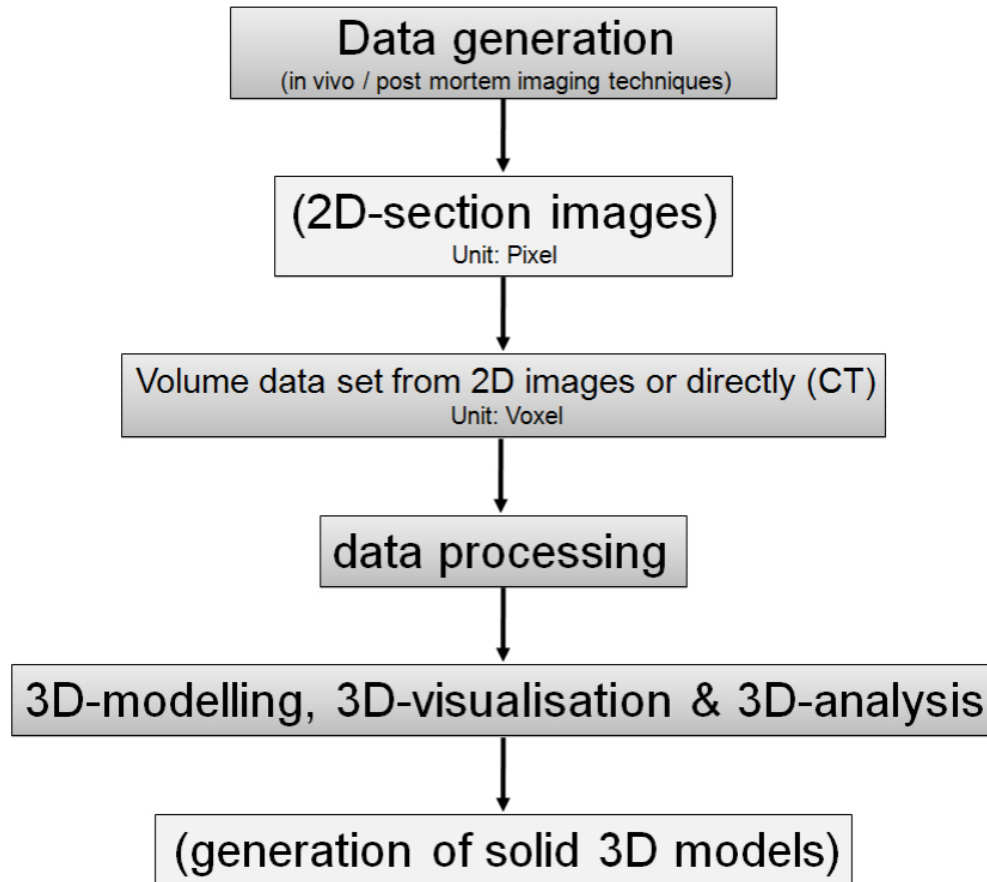(generation of solid 3D models)

**Fig. (2).** Steps involved in constructing three-dimensional (3D) models; common to all modern 3D imaging methods. Note that helical or spiral computed tomography directly constructs a volume data set.

the edge lengths of a Pixel (squares or rectangles that compose a digital 2D image) and Z is the distance between two subsequent sections (Fig. **3**).

The size of a voxel is a measure for the resolution of a volume data set. However, due to interpolation errors and similar artefacts inevitably introduced during data genera-

tion, this does not mean that structures as small as one voxel can be really detected. A simple example, a spherical cell with a diameter of 15 μm might be missed in a volume data set with a voxel size (resolution) of 15 μm x 15 μm x 15 μm (Fig. **4**). Even if the cell would be clearly assigned to one voxel, it is doubtful whether the occupied voxel (to which
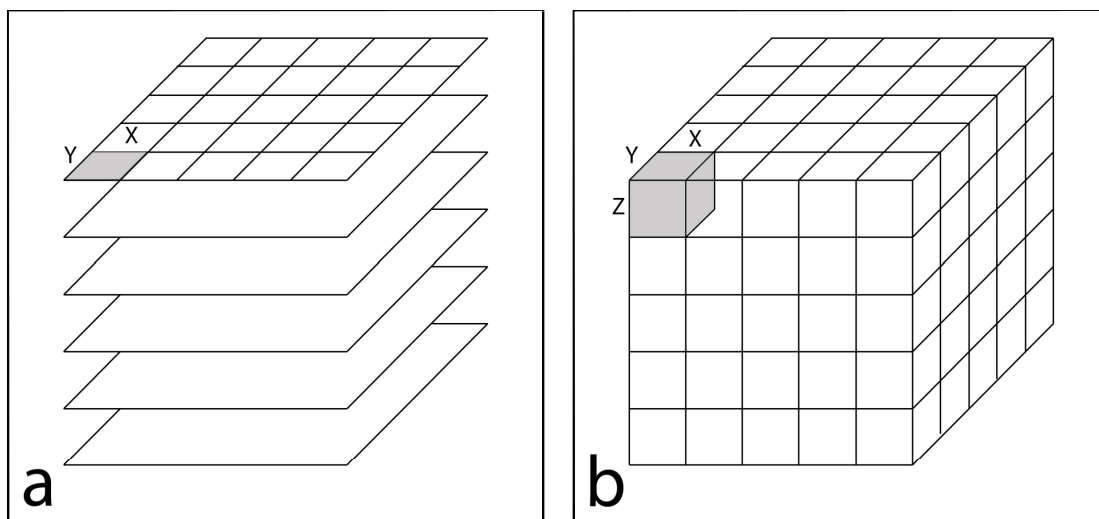


**Fig. (3).** Volume data set. (**a**) Two-dimensional (2D) images consisting of single pixels are stacked together. (**b**) A volume data set results. It is composed of voxels. The x-axis (X) and y-axis (Y) dimensions of a voxel are the x- and y-dimensions of the pixel. The section thickness or distance between subsequent section images represents the z-axis dimension (Z) of the voxel.

only one certain colour or grey scale value can be assigned) really represents a cell. No information at all is available about the morphology of the cell. Information about a space covered by 5 x 5 x 5 voxels is necessary for being able to, at least roughly, define cell morphology. In our example, a voxel size of 3 μm x 3 μm x 3 μm would be necessary to detect whether the cell is spherical or not (Fig. **4**). Data generation artefacts, such as interpolation errors, partial volume effects, or bad data quality (low signal/noise ratio, blurring of fluorescence signals) usually obscure image information. Therefore even higher resolutions are required for classifying single cells three dimensionally.

Mouse embryos and fetus are small biological objects. Even if no cellular information is required, it is necessary to produce volume data sets of high resolution to properly ana-
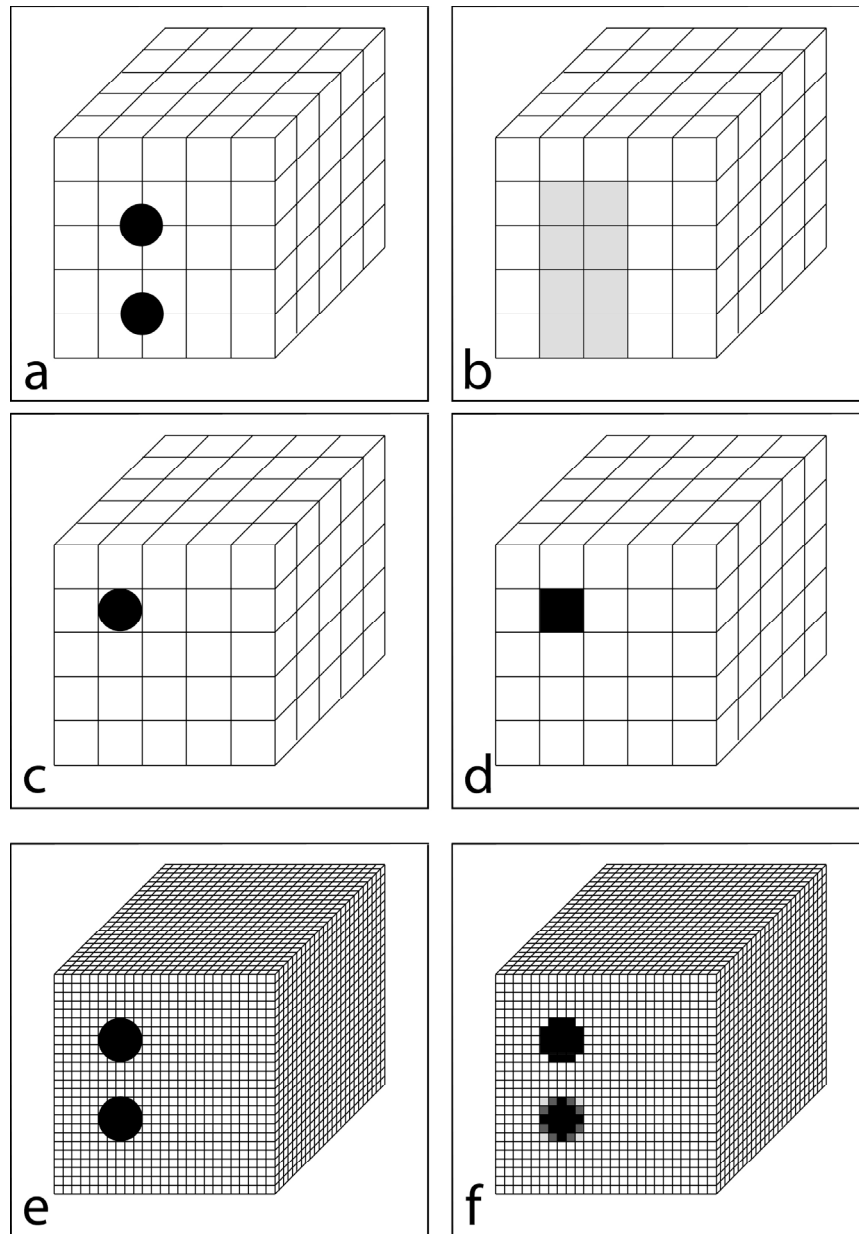


**Fig. (4).** Consequence of volume data resolution. Left panels show to which position within a volume data set spherical cells, which have a diameter of 15 μm and are sectioned at their equator, would be captured. Corresponding right panels show the digital representation of the cell in a section through the volume data set. Voxel size in a-d is 15 μm x 15 μm x 15 μm, voxel size in e and f is 3 μm x 3 μm x 3 μm. (**a**) 2D sections of two cells. They would project to cross points of neighbour voxels. (**b**) If captured in a grey-scale data generation mode the sections of the cells are represented as grey areas. Note that the 2 cells of 15 μm diameter appear as a 8 pixel (120 μm) long and 4 pixel (60 μm) broad structure. If the cells are captured in a binary data generation mode, they do not have any representation in the volume data set. (**c**) A cell would project exactly to a voxel. (**d**) The cell is detected and represented by a voxel. Note that shape information is entirely lost. (**e**) In volume data of higher resolution (3 μm x 3 μm x 3 μm instead of 15 μm x 15 μm x 15 μm), the 2D section through the equator of cells of a diameter of 15 μm would project to an area of 25 pixels (**f**) In the volume data set the section through the cell is represented by 21 pixels – if generated in a binary modus (top cell). A cell appears differently if captured in a grey-scale modus (bottom cell). Note that the two cells can be clearly distinguished and that they appear roundish.

lyse anatomical details and tissue architecture. This is especially true if the tissue layers of the heart or the three dimensionally complex trees of blood vessels should be reconstructed (In late mouse embryos and early mouse fetus even the diameter of large vascular channels, such as the great intrathoracal arteries is only approximately 30 to 100 µm.).

The accuracy and resolution and thus the usability, and significance of 3D models almost entirely depend on the quality and the characteristics of the underlying volume data set. The characteristics of a volume data set depend on the quality of the primary 2D images. It is therefore essential to carefully choose which imaging modality is to be used for data generation.

In contrast, the process of creating 3D models from volume data sets is essentially independent from the imaging modality employed for volume data generation. A number of commercially (e.g. Amira (Mercury systems), Volocity (Improvision), Maya (Autodesk, www.autodesk.com/maya)), or freely (e.g. SurfDriver, S. Lozanoff, University of Hawaii, D. Moody, University of Alabama; Osirix, www.osirix-viewer.com) available software packages exist for this task. All of them feature similar image processing and visualisation tools.

In the following, we will briefly describe and discuss the various image modalities, which can be used for generating volume data sets of a resolution which is high enough to permit 3D visualisation and 3D analysis of the cardiovascular system of unborn mice.

### IN VIVO VOLUME DATA GENERATION METHODS

6-14 mouse embryos develop inside the two horns of the mouse uterus. Since they are rather small, thickly surrounded by maternal tissues, and float or move in amnion fluid, *in vivo* visualisation of mouse embryos/fetus is very difficult. Even more difficult is the *in vivo* 3D visualisation of their cardiovascular system. The cardiovascular system is composed of a lot of particularly small components, which due to the heart beat and rapid heart frequency quickly change in size and position.

Though a lot of imaging methods exist that permit *in vivo* visualisation of biological specimens, some of them (e.g. near infrared imaging techniques, optical coherence, polarised light spectroscopy) [33-36], cannot be used for imaging (not even two-dimensionally) unborn mice. *In vivo* imaging techniques, which permit 2D *in utero* analysis of mouse embryos or fetus, and in principle could be used for the generation of volume data, are briefly discussed below.

### In Vivo Micro- Magnetic Resonance Imaging (µMRI)

Attempts were made to use MRI for 3D visualisation of living embryos of various species [37-40] However, up to now µMRI is unable to provide volume data in a resolution and quality, which is sufficient for visualising the cardiovascular system of mouse embryos or mouse fetus *in utero*.

### In Vivo (Micro-) Computed Tomography ((µ)CT)

CT detects different tissues of biological objects by their permeability for X-rays. Therefore it allows to distinguish tissues by their density. But embryonic and fetal tissues - except for ossified tissue - are relatively homogeneous. Con-sequently the contrasts between most tissues are very low in CT scans. Enhancing the contrast with the aid of contrast agents is almost impossible in living mouse embryos and fetus. Therefore, *in vivo* CT might be used for analysing ossification centres in mouse fetus and late non-mammal embryos [41]. However it is insufficient for *in vitro* 3D visualisation of mouse embryos and soft tissues of mouse fetus.

### Ultrasound (US)

For mouse embryos, 2D (B-mode) ultrasound can be - and is - used for analysing heart morphology and blood flow in the late fetal and perinatal period [42, 43]. For human fetus ultrasound data can be even used for creating 3D models of various fetal structures [44-49].

However *in vivo* 3D visualisation of the cardiovascular-system of living mouse embryos with the aid of ultrasound is currently impossible.

### POST-MORTEM VOLUME DATA GENERATION METHODS

Currently *in vivo* imaging methods are unable to assist 3D analysis of the cardiovascular phenotype of mouse embryos/fetus. In contrast most *post mortem* imaging techniques are successful in providing 3D phenotype information on different levels of detail. Some of these methods even are capable of providing 3D information on gene expression patterns in the context of tissue architecture and embryo anatomy.

Following steps are common to all *post mortem* imaging techniques: Mouse embryos/fetus are allowed to develop *in utero*, until the pregnant mice have reached the assigned day of pregnancy. At this day the dams are sacrificed, the uterus is opened, and the embryos or fetus are harvested. They either are staged according to the duration of embryo development (day post conceptionem, dpc) or according to external features [13]. After harvesting and staging the embryos are processed according to protocols that are specific for the technique, which will be used for subsequent volume data generation.

Several methods exist for *post mortem* 3D imaging of sacrificed mouse embryos/fetus. Each of the methods produces data of different accuracy, quality, and resolution and is optimised for specific scientific applications. The methods can be grouped in two – "non destructive" and "destructive" methods. The methods of the first group ("non destructive" methods) produce volume data without destroying the specimen. In contrast, "destructive" methods produce volume data while physically sectioning and thus destroying the specimen. Information and data obtained by analysing an embryo or fetus with a non-destructive method can be combined with data and information generated from the same embryo with the aid of a destructive imaging method. An example is the µMRI-HREM pipeline [50].

### NON DESTRUCTIVE 3D IMAGING METHODS

### Micro-Magnetic Resonance Imaging (µMRI)

*Post mortem* µMRI or MRM (magnetic resonance microscopy) is well suited for generating volume data sets from sacrificed mouse fetus, in which tissue contrasts are enhanced with unspecific contrast enhancing agents [51, 52].

After fixation the fetus are stored in dimeglumine gadopentetate (Gd-DTPA, Magnevist) or ProHance (gadoteridol, Bracco Diagnostics) for a few days, before they are embedded in agarose. Then they are scanned either with a high-Teslar MRI apparatus (up to 11.7 T), or specific laboratory animal scanners. In principle µMRI also suits for analysing mouse embryos. However the resolution of the produced volume data sets is too low to permit thorough 3D analysis of their developing cardiovascular system.

µMRI usually produces images with total side dimensions of 128 x 128, 256 x 256, 512 x 512 (routine) or 1024 x 1024 Pixel. In images with such a relative small image size, partial volume effects (voxels can represent more than one tissue type) may have dramatic effects. This lowers the significance of a volume data set generated from MRI data [53]. A second problem is the disadvantageous signal to noise ratio in high resolution MRI scans. Therefore lowering the dimension of a voxel below approximately 10 µm x 10 µm x 10 µm does not

bring forth new information [52]. The third problem is that up to now no routinely applicable techniques exist, which permit the specific labelling of tissues or gene products – although attempts exist [54, 31].

Despite its disadvantages µMRI is an important tool in modern biomedical research. Thanks to the possibility to scan up to 32 specimens in an overnight run [55, 56], µMRI is used in mutagenesis studies to screen the phenotype of prenatally lethal offspring of randomly produced mouse mutants. (Such mutants are the result of large scale mutagenesis experiments devoted to detecting new mouse models for hereditary diseases [5, 8, 57-63]). Although µMRI fails to detect small cardiac and vascular malformations in early mouse fetus [50], its yet unmatched speed and the possibility to detect potentially lethal malformations (Fig. **5**), justifies its application in mutagenesis screens. In any case, secondarily to µMRI scanning scanned and suspect specimens can be further analysed with the aid of destructive imaging tech-
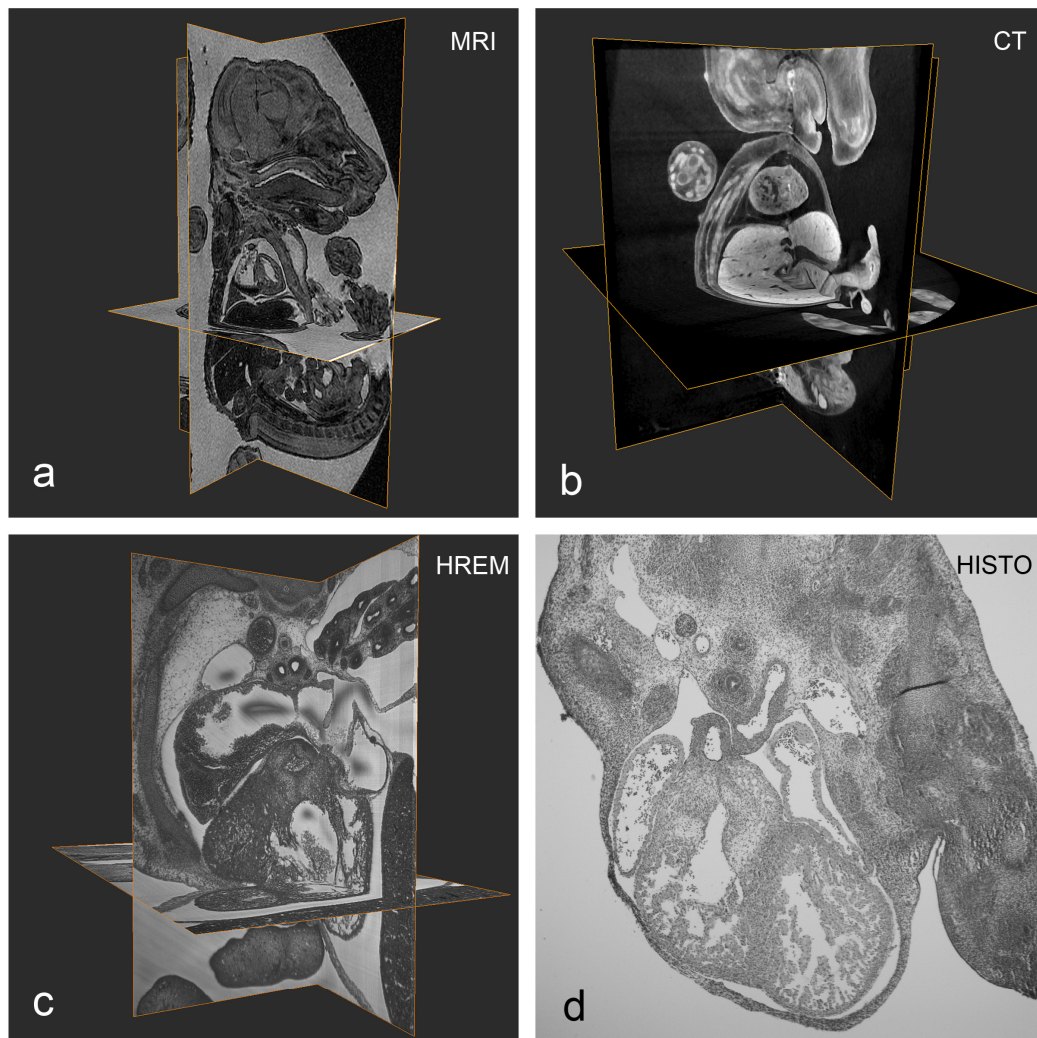


**Fig. (5).** Exemplary data generated with various *post mortem* volume data generation methods. (**a**) Original section plane and 2 perpendicularly arranged virtual section planes through µMRI data of a 15.5 dpc mouse fetus. Voxel size: 25.5 µm x 25.5 µm x 24.5 µm. (**b**) Original section plane and 2 perpendicularly arranged virtual section planes through µCT data of a 13.5 dpc mouse embryo. Voxel size: 9 µm x 9 µm x 9 µm: (**c**) Original section plane and 2 perpendicularly arranged virtual section planes through HREM volume data of a 14.5 dpc mouse fetus. Voxel size: 1.07 µm x 1.07 µm x 2 µm. (**d**) Hematoxylin/eosin stained histological section through a 15.5 dpc mouse fetus. Pixel size: 1.13 µm x 1.13 µm.

niques [50].

### *Post Mortem* Micro Computed Tomography (µCT)

While *in vivo* µCT is not of much use for visualising the cardiovascular system of mouse embryos/fetus, *post mortem* µCT is a powerful tool. For two reasons *post mortem* µCT analysis of embryos and fetus is more promising than their *in vivo* µCT analysis: Firstly, the tissues of harvested embryos can be unspecifically contrasted with osmiumtetroxide. Secondly the cardiovascular system can be perfused with hardening contrast agents prior to scanning.

Osmiumtetroxide staining and subsequent µCT scanning of mouse embryos is an already established tool, which is also termed as "virtual histology" [64]. The term "virtual histology" is misleading, since the quality of the produced scans is far away from the quality of digital images of histological sections. Also the resolution of the volume data (8 µm x 8 µm x 8 µm) is comparably low. Nevertheless the technique permits precise descriptions of the shape and even the tissue layers of some organs (Fig. **5**) such as the heart within relative short data generation times [65, 66]. A profitable increase of resolution might be possible within the next years.

Perfusion of the cardiovascular system of embryos and fetus with x-ray dense substances and subsequent CT scanning is an interesting and promising new approach that permits qualitative and quantitative analysis of the lumina of hearts and blood vessels. Although developed for chick embryos [67] and not yet tested in the mouse, it seems to be only a question of time until it will also be applied for the latter. After harvesting, a x-ray dense substance is injected into the cardiovascular system of the specimen. This substance hardens and is not altered (does not shrink) during further embryo processing. If the substance is administered with a physiological pressure, the cavitates and lumina of the heart and blood vessels can not only be topologically analysed, but even their true dimensions can be measured. However, a problem remains with analysing the walls of blood vessels or the anatomy of other embryonic organs, because, although heart and blood vessel lumina are perfectly contrasted all the embryonic tissues are not.

Currently µCT is unable to provide 3D information of gene expression and gene product patterns. However, the development of such a method seems to be possible and efforts now at hand.

### Optical Projection Tomography (OPT)

OPT was introduced 2002 by James Sharp [68] (see also http://genex.hgu.mrc.ac.uk/OPT_Microscopy/optwebsite/frontpage/index.htm) and became an immediate success [69-75]. Within a few years it was commercialised and relatively easy to handle OPT scanners can be purchased from several companies.

For OPT scanning, embryos must be immersed in benzyl alcohol / benzyl benzoate to become translucent. Then they are embedded in agarose, before they are mounted on the OPT apparatus. Like with MRI and CT, the embryos are scanned segment by segment to create subsequent digital section images. Creating such a section image, involves stepwise rotation of the embryo and transmission of light (instead of x-rays) through the embryo segment (Alternatively monochrome light is used to excite the tissues at the segment.). The light passing through the specimen, respectively the light emitted from the excited tissues is detected by a camera and this information is used for reconstructing a digital section image. After generating such a section image, the embryo is shifted and a similar image of the next embryo segment is generated. The aligned digital images are stacked together to build up a volume data set.

OPT is the only non-destructive imaging method, which permits the 3D analysis of specifically labelled gene expression and gene product patterns in relative high resolution (5 µm x 5 µm x 5 µm). Using "fluorescence OPT" (eOPT), even multiple gene expression patterns can be visualised simultaneously. Although the scans are not of the appearance of histological images, the resolution and the quality of OPT data is sufficient for analysing anatomical details of the cardiovascular system. For eliminating the artefacts introduced by data generation, a number of sophisticated mathematical methods were recently published [76, 77].

One of the problems of OPT is that data can only be created from translucent, whole mount stained specimens. This sets an upper specimen size limit. Mouse embryos, especially early embryos are small enough to become 3D visualised with OPT [73, 78-80]. Late mouse embryos and mouse fetus must be parted or dissected prior to staining and scanning (e.g. the hearts must be isolated) to produce sufficiently good results in respect to anatomy and gene expression patterns. Another serious problem of OPT, which especially complicates 3D visualisation of the cardiovascular system is caused by blood cells remaining inside the cardiac chambers and the blood vessels. Information of embryo morphology is best obtained by using tissue autofluorescence provoked by using GFP and RFP filter sets. However under these conditions blood cells show intense auto-fluorescence, which obscures anatomical information and introduces artefacts.

Very recently the spectrum of OPT was expanded to *in vivo* 3D and four-dimensional (4D) imaging of the limbs of explanted and cultured mouse embryos [81]. Although not yet out of its child's shoes, this is an innovative and very powerful approach. However, since it currently does not permit 4D analysis of the cardiovascular system, we will not discuss it further in this paper.

### Surface Electron Microscopy (SEM)

SEM images the surface of fixed, dehydrated, dried, and coated specimens.

SEM has been used to study the morphology of embryonic structures of various species [82-85]. Alternatively it can be used in combination with corrosion casting for analyzing small vascular networks, such as capillary beds [86, 87]. However SEM produces merely pseudo 3D images and can not be used for generating digital volume data. Therefore it is not further discussed in this review.

## DESTRUCTIVE IMAGING METHODS

### Corrosion Casts

An ancient, but still often used technique for 3D visualisation of the topology and branching patterns of blood ves-

sels is the creation of corrosion casts [88-90]. Dyed and liquid plastics are injected into the cardiovascular system of embryos. After hardening, all tissues surrounding the plastic are corroded and a physical 3D model of the blood vessel lumina remains.

This sophisticated and powerful technique permits detailed 3D analysis of the systematic and the branching patterns of the lumen of blood vessels. However it is also restricted to such analysis. It does not generate digital volume data sets, which can be used for creating virtual 3D models and does not permit the visualisation of embryonic tissues. Therefore we will not discuss it further in this paper.

**Histological Section Based Techniques**

Modern methods that generate virtual 3D models from a series of subsequent histological sections through an embryo follow a simple workflow. An embryo is harvested and then infiltrated with and embedded in wax or resin. The block of embedding medium containing the embryo is sectioned on a microtome. The sections are collected, stretched in a water bath and mounted on glass slides. After removing the embedding medium (wax only) the mounted sections are unspecifically or specifically contrasted with histochemical, immunohistochemical, or in situ hybridisation techniques, and cover slipped (Alternatively whole mount staining techniques can be used prior to the embedding of the specimens). A light microscope, equipped with a digital camera, or a scanner are now used for capturing digital images of each histological section (Fig. **5**). All digital section images of a series are then aligned according to either intrinsic or fiducial marker [91]. Then they are virtually stacked together and converted to a volume data set, which can be processed and three dimensionally visualised and analysed. Several problems complicate this approach:

1.   *Missing sections and distortions:* Histological sections must be collected, stretched on a water bath and mounted on glass slides. Especially if resin sections are collected between 1% and 10% of the sections of a series and the information enclosed in them is lost. Furthermore, a number of artefacts are introduced by sectioning, section mounting, and section processing. Such artefacts are for example section shrinkage, non-affine distortions, and inhomogeneous tissue staining within or between sections.

2.   *Alignment:* It is necessary to align the histological sections with the aid of cross tables on the microscope to allow capturing of matching parts of subsequent sections and to keep a field of view as large as possible. But despite this alignment the digital section images are not aligned properly. Thus re-alignment of the digital images of the sections is an additional and crucial step of all histological section based methods. Several alignment methods exist. Widely used are the so called "best fit" or "best guess" methods and intrinsic marker techniques [92-96]. But these methods are subjectively biased and produce questionable results of doubtful quality. A different approach that ensures objective alignment of digital section images is their alignment with the aid of fiducial markers [97-99]. But for introducing fiducial markers resolution has to be sacrificed and an additional, time expensive image processing step, namely marker segmentation is required.

3.   *Time and personnel expense:* Histological sections must be manually generated, collected and mounted on glass slides. Then they must be stained, cover slipped, and cleaned. The next step, image capturing, involves that they are placed, one by one under a light or fluorescence microscope and rotated until they at least roughly match the field of view (This step might be speeded up by using digital scanners and automated slide mounters). 180 degrees rotated as well as flipped sections must be identified and corrected. Subsequently each single digital image has to be aligned with the aid of special software tools. Each of these steps is time expensive and must be conducted by specialists.

4.   *Section thickness:* The resolution of the digital 2D image of a histological section can be kept very high. However, the resolution and usability of a volume data set on the basis of 2D sections depends not only on the resolution of the 2D sections. It also depends on the thickness of each section. For a number of technical reasons the thickness of histological wax sections is between 5 µm and 10 µm. This limits the resolution of a volume data set generated from such sections. If section thickness is e.g. 5 µm, only volume data with a minimal resolution of (X µm x Y µm x 5 µm) can be created (X µm x Y µm means the Pixel dimension of the 2D image). In such volume data, e.g. branching of capillaries (approximate diameter of 5 µm), and the correct course of small blood vessels might be missed.

Despite the many disadvantages, histological section based 3D imaging techniques also have some major advantages:

1.   A great number of tested protocols exist for visualising gene expression and gene product patterns in histological sections. Even better, the possibility to split a section series into two or three offers the possibility to stain different gene products and merge the results in one volume data set [100]. Such a splitting however causes a loss in resolution, since the distance between two sections doubles or triples (see last paragraph).

2.   If necessary, physical sections can be re-studied in a higher resolution or even stained with additional agents.

3.   The production of histological sections needs only the basic equipment of biomedical laboratories.

For special scientific questions, histologcial section based 3D imaging techniques are still the method of choice. However, their many disadvantages, especially the enormous time and personnel expense effectively prevent their application in daily routine.

**3D Confocal Imaging**

Confocal imaging theoretically can be used for *in vivo* analysis of very early explanted and cultured mouse embryos. However, in the praxis, it is/was only used for 3D

imaging of living transparent fish and frog embryos [26, 101-103], but not for the cardiovascular system of mouse embryos.

Confocal imaging plays an important role as a *post mortem* 3D imaging method. Embryos are embedded in resin and sectioned into 50 - 100 μm thick sections. The sections are stained with antibodies coupled with fluorochromes. Mono-chrome light is directed either episcopically, or from the side towards the section in order to excite the tissues and/or fluorochromes at a narrow segment of the section. The ex-cited fluorochromes and tissues emit fluorescence and auto-fluorescence signals which are detected with a digital camera sitting on a microscope. Thanks to a system of pinholes in front of the objective only signals coming from a very nar-row focus plane passes to the camera. Such digital images of subsequent optical sections can be created from the physical section. The digital images are perfectly aligned and can be immediately converted into a volume data set.

The main problem of confocal microscopy is that signals emitted from tissues, which are located deep inside the physical section are weaker than signals emitted from the same tissues located on the surface of the physical section. The reason is that light emitted from a deep optical section plane has to travel through parts of the sectioned embryo. When it has reached the surface of the physical section it is already partly absorbed and thus extinguished by the overly-ing tissues. The use of calibration beads and sophisticated mathematical tools ("deconvolution" filters) eliminate or at least reduce this artefact [104, 105]. However, from a certain distance onwards signals can be totally extinguished by over-lying tissues. Thus the depth of optical sectioning is limited to approximately 50-100 μm.

Due to this absorption, of signals by overlying tissues, volume data created with the confocal technique cannot exceed 50-100 μm in the z-direction. This is too small for generating useful 3D models of the cardiovascular system of whole mouse embryos. It is however sufficient for 3D analy-sis of the expression patterns of multiple, selectively labelled (trans-)genes in small parts of embryos [106, 107], or the morphology of cells in the walls of the heart and blood ves-sels.

**Table 1. Techniques Suitable for Imaging the Cardiovascular System of Mouse Embryos/Fetus**

| | Min. Voxel Size (Reasonable Quality) | Main Advantages | Main Drawbacks | Detection of Gene Expression? | Key References |
|---|---|---|---|---|---|
| *In vivo* | | | | | |
| (MRI) | $(25^3 \ \mu m^3)$ $100^3 \ \mu m^3$ | good tissue contrasts | low resolution movement artefacts | no | [37, 38] |
| (CT) | not yet established for mouse embryos | good visualisation of ossification | low tissue contrast movement artefacts | no | |
| (US) | | visualisation of blood flow | low contrast no proper volume data | no | [42, 43] |
| *Post mortem (non destructive)* | | | | | |
| μMRI | $10^3 \ \mu m^3$ | high-throughput screening | partial volume effects high noise/signal ratio | no | [51, 52, 55] |
| μCT | $8^3 \ \mu m^3$ | short data generation time | low tissue contrasts | no | [64, 65, 66] |
| OPT | $5^3 \ \mu m^3$ | simultaneous analysis of multiple gene expression patterns | transparents specimens required specimen size limitation whole mount staining required | yes | [68] |
| *Post mortem (destructive)* | | | | | |
| histological section series | 0.3 μm x 0.3 μm x 7 μm | established method tripartition of series | laborious & time expen-sive section processing arte-facts | yes | [94, 96, 98] |
| confocal technique | $0.3^3 \ \mu m^3$ | subcellular structures in good quality | limited light penetration distance transparent specimens required | yes | [101, 106] |
| episcopic imaging | 0.5 μm x 0.5 μm x 1 μm | simple cheap | whole mount staining required shining through artefacts | yes (not all) | [108-112, 114] |

Although the table lists the most promising "*in vivo* techniques", none of them currently enables the generation of useful volume data of the heart and great blood vessels of unborn mice. Note that each of the listed *post mortem* techniques has its specific advantages and disadvantages. It entirely depends on the scientific question, which technique is the most adequate.

**Episcopic Imaging Methods**

3D episcopic or "block face" imaging creates volume data from histologically embedded and physically sectioned embryos. The specimens are embedded in wax or resin mixtures. The blocks of embedding medium containing the specimens are mounted and sectioned on a microtome. After each cut a digital image showing the surface of the block is captured with the aid of a digital camera sitting on the photo-tubus of a magnifying optic. Since the images are captured at reproducible photo-positions, the digital images are aligned and can be immediately stacked together and converted to a volume data set. Several methods exist for generating volume data sets on the basis of the episcopic imaging technique [108-112]. Each has its advantages and disadvantages. For a detailed review on episcopic 3D imaging techniques see [113].

In contrast to histological section based techniques, 3D episcopic imaging techniques create volume data from digital images showing the unsectioned specimen, while it becomes sectioned. Therefore stacks of hundreds to thousands of aligned digital images (typically between 600 and 2000) are available immediately after sectioning, which is performed in an automated way and lasts only a few hours. Data generated with episcopic 3D imaging techniques can be of almost histological quality (compare e.g. Fig. **5** and http://www.meduniwien.ac.at/3D-Rekonstr/HREM/), but without showing section mounting, section staining, section processing, and alignment artefacts – as digital images series created from histological sections do.

Episcopic imaging techniques are capable of generating volume data with voxel sizes as low as 1 $\mu m^3$. The morphology and tissue architecture of all the components of the cardiovascular system of all developmental stages of mouse embryos can be 3D visualised in high resolution [50, 111]. Taking advantage of whole mount in situ hybridisation and whole mount staining, a few episcopic methods permit the 3D visualisation of gene expression and gene product patterns in respect to the cardiovascular system of mouse embryos/fetus [114]. However, in specimens the thickness of which exceeds a few hundred $\mu m$, whole mount staining cannot be performed in good quality. Therefore, 3D analysis of gene expression patterns in mouse fetus requires the dissection of the specimens and their analysis in parts (e.g. thorax only).

**CONCLUSION**

Currently *in vivo* 3D imaging of the cardiovascular system of mouse embryos and mouse fetus does not provide convincing results. The greatest potential for detailed 3D analysis of the cardiovascular system of mouse embryos and mouse fetus have destructive *post mortem* imaging methods. However, for comprehensive 3D visualisation of the embryonic and fetal heart and vasculature, the future lays in the combination of non-destructive and destructive imaging methods (see Table **1**).

**ACKNOWLEDGEMENTS**

**REFERENCES**

[1]     Pierpont ME, Basson CT, Benson DW, Jr., *et al.* Genetic basis for congenital heart defects: current knowledge: a scientific statement from the American Heart Association Congenital Cardiac Defects Committee, council on cardiovascular disease in the young: endorsed by the American Academy Of Pediatrics. Circulation 2007; 115: 3015-38.

[2]     Friedel RH, Plump A, Lu X, *et al.* Gene targeting using a promoter-less gene trap vector ("targeted trapping") is an efficient method to mutate a large fraction of genes. Proc Natl Acad Sci USA 2005; 102: 13188-93.

[3]     Fire A, Xu S, Montgomery MK, Kostas SA, Driver SE, Mello CC. Potent and specific genetic interference by double-stranded RNA in *Caenorhabditis elegans*. Nature 1998; 391: 806-11.

[4]     Hammond SM, Caudy AA, Hannon GJ. Post-transcriptional gene silencing by double-stranded RNA. Nat Rev 2001; 2: 110-9.

[5]     Herron BJ, Lu W, Rao C, *et al.* Efficient generation and mapping of recessive developmental mutations using ENU mutagenesis. Nat Genet 2002; 30: 185-9.

[6]     Brown SD, Hardisty RE. Mutagenesis strategies for identifying novel loci associated with disease phenotypes. Semin Cell Dev Biol 2003; 14: 19-24.

[7]     Beckers J, Hoheisel J, Mewes W, Vingron M, Hrabe de Angelis MH. Molecular phenotyping of mouse mutant resources by RNA expression profiling. Curr Genomics 2002; 3: 121-9.

[8]     Seltmann M, Horsch M, Drobyshev A, Chen Y, de Angelis MH, Beckers J. Assessment of a systematic expression profiling approach in ENU-induced mouse mutant lines. Mamm Genome 2005; 16: 1-10.

[9]     Reecy JM, Spurlock DM, Stahl CH. Gene expression profiling: insights into skeletal muscle growth and development. J Anim Sci 2006; 84(Suppl): E150-4.

[10]    Mitiku N, Baker JC. Genomic analysis of gastrulation and organogenesis in the mouse. Dev Cell 2007; 13: 897-907.

[11]    Niemann H, Carnwath JW, Kues W. Application of DNA array technology to mammalian embryos. Theriogenology 2007; 68 (Suppl 1): S165-77.

[12]    Zhu H, Cabrera RM, Wlodarczyk BJ, *et al.* Differentially expressed genes in embryonic cardiac tissues of mice lacking Folr1 gene activity. BMC Dev Biol 2007; 7: 128.

[13]    Theiler K. The house mouse: development and normal stages from fertilizatioin to 4 weeks of age. Berlin: Springer-Verlag 1972.

[14]    Born G. Die Plattenmodelliermethode. Arch Mikr Anat 1883; 22: 584-99.

[15]    His W. Anatomie menschlicher Embryonen. III. Zur Geschichte der Organe. Leipzig 1885.

[16]    His W. Über die methoden der plastischen rekonstruktionund über deren bedeutung für anatomie und entwicklungsgeschichte. Anatomischer Anzeiger 1887; II: 382-94.

[17]    Hopwood N. Embryos in wax: models from the Ziegler studio: Whipple Museum of the History of Science 2002.

[18]    Schook P, Blom N. A three-dimensional reconstruction method preserving light microscopic and transmission electron microscopic information. Acta Morphol Neerl Scand 1978; 16: 157-70.

[19]    Stephens PR. Three-dimensional reconstructions of a cavity using plastic sheet and modelling clay. J Microsc 1979; 115: 175-80.

[20]    Prothero JW, Tamarin A, Pickering R. Morphometrics of living specimens: a methodology for the quantitative three-dimensional study of growing microscopic embryos. J Microsc 1974; 101: 31-58.

[21]    Prothero J, Prothero J. Three-dimensional reconstruction from serial sections. I: a portable microcomputer-based software package in Fortran. Comput Biomed Res 1982; 15: 598-604.

[22]    Huijsmans DP, Lamers WH, Los JA, Strackee J. Toward computerized morphometric facilities: a review of 58 software packages for computer-aided three-dimensional reconstruction, quantification, and picture generation from parallel serial sections. Anat Rec 1986; 216: 449-70.

[23]    Paulus MJ, Gleason SS, Kennel SJ, Hunsicker PR, Johnson DK. High resolution X-ray computed tomography: an emerging tool for small animal cancer research. Neoplasia 2000; 2: 62-70.

[24]    Foster FS, Zhang MY, Zhou YQ, *et al.* A new ultrasound instrument for *in vivo* microimaging of mice. Ultrasound Med Biol 2002; 28: 1165-72.

[25]    Chapon C, Franconi F, Roux J, Le Jeune JJ, Lemaire L. Prenatal evaluation of kidney function in mice using dynamic contrast-

enhanced magnetic resonance imaging. Anat Embryol (Berl) 2005; 209: 263-7.

[26] Liebling M, Forouhar AS, Wolleschensky R, *et al.* Rapid three-dimensional imaging and analysis of the beating embryonic heart reveals functional changes during development. Dev Dyn 2006; 235: 2940-8.

[27] Bain MM, Fagan AJ, Mullin JM, McNaught I, McLean J, Condon B. Noninvasive monitoring of chick development in ovo using a 7T MRI system from day 12 of incubation through to hatching. J Magn Reson Imaging 2007; 26: 198-201.

[28] Johnson KA. Imaging techniques for small animal imaging models of pulmonary disease: micro-CT. Toxicol Pathol 2007; 35: 59-64.

[29] Lee SC, Mietchen D, Cho JH, *et al. In vivo* magnetic resonance microscopy of differentiation in *Xenopus laevis* embryos from the first cleavage onwards. Differentiation 2007; 75: 84-92.

[30] Wessels JT, Busse AC, Mahrt J, Dullin C, Grabbe E, Mueller GA. *In vivo* imaging in experimental preclinical tumor research--a review. Cytometry A 2007; 71: 542-9.

[31] Deans AE, Wadghiri YZ, Berrios-Otero CA, Turnbull DH. Mn enhancement and respiratory gating for in utero MRI of the embryonic mouse central nervous system. Magn Reson Med 2008; 59: 1320-8.

[32] Sun L, Lien CL, Xu X, Shung KK. *In vivo* cardiac imaging of adult zebrafish using high frequency ultrasound (45-75 MHz). Ultrasound Med Biol 2008; 34: 31-9.

[33] Welzel J. Optical coherence tomography in dermatology: a review. Skin Res Technol 2001; 7: 1-9.

[34] Ntziachristos V, Bremer C, Weissleder R. Fluorescence imaging with near-infrared light: new technological advances that enable *in vivo* molecular imaging. Eur Radiol 2003; 13: 195-208.

[35] Wolfberg AJ, du Plessis AJ. Near-infrared spectroscopy in the fetus and neonate. Clin Perinatol 2006; 33: 707-28.

[36] O'Doherty J, Henricson J, Anderson C, Leahy MJ, Nilsson GE, Sjöberg F. Sub-epidermal imaging using polarized light spectroscopy for assessment of skin microcirculation. Skin Res Technol 2007; 13: 472-84.

[37] Jacobs RE, Fraser SE. Magnetic resonance microscopy of embryonic cell lineages and movements. Science 1994; 263: 681-4.

[38] Hogers B, Gross D, Lehmann V, *et al.* Magnetic resonance microscopy of mouse embryos in utero. Anat Rec 2000; 260: 373-7.

[39] Louie AY, Huber MM, Ahrens ET, *et al. In vivo* visualization of gene expression using magnetic resonance imaging. Nat Biotechnol 2000; 18: 321-5.

[40] Ahrens ET, Srinivas M, Capuano S, Simhan HN, Schatten GP. Magnetic resonance imaging of embryonic and fetal development in model systems. Methods Mol Med 2006; 124: 87-101.

[41] Guldberg RE, Lin AS, Coleman R, Robertson G, Duvall C. Micro-computed tomography imaging of skeletal development and growth. Birth Defects Res C Embryo Today 2004; 72: 250-9.

[42] Shen Y, Leatherbury L, Rosenthal J, *et al.* Cardiovascular phenotyping of fetal mice by noninvasive high-frequency ultrasound facilitates recovery of ENU-induced mutations causing congenital cardiac and extracardiac defects. Physiol Genomics 2005; 24: 23-36.

[43] Yu Q, Leatherbury L, Tian X, Lo CW. Cardiovascular assessment of fetal mice by in utero echocardiography. Ultrasound Med Biol 2008; 34: 741-52.

[44] Meyer-Wittkopf M, Cooper S, Vaughan J, Sholler G. Three-dimensional (3D) echocardiographic analysis of congenital heart disease in the fetus: comparison with cross-sectional (2D) fetal echocardiography. Ultrasound Obstet Gynecol 2001; 17: 485-92.

[45] Mittermayer C, Blaicher W, Deutinger J, Bernaschek G, Lee A. Prenatal diagnosis of a giant foetal lymphangioma and haemangiolymphoma in the second trimester using 2D and 3D ultrasound. Ultraschall Med 2003; 24: 404-9.

[46] Mittermayer C, Blaicher W, Brugger PC, Bernaschek G, Lee A. Foetal facial clefts: prenatal evaluation of lip and primary palate by 2D and 3D ultrasound. Ultraschall Med 2004; 25: 120-5.

[47] Avni FE, Cos T, Cassart M, *et al.* Evolution of fetal ultrasonography. Eur Radiol 2007; 17: 419-31.

[48] Tutschek B, Sahn DJ. Three-dimensional echocardiography for studies of the fetal heart: present status and future perspectives. Cardiol Clin 2007; 25: 341-55.

[49] Yagel S, Cohen SM, Shapiro I, Valsky DV. 3D and 4D ultrasound in fetal cardiac scanning: a new look at the fetal heart. Ultrasound Obstet Gynecol 2007; 29: 81-95.

[50] Pieles G, Geyer SH, Szumska D, *et al.* microMRI-HREM pipeline for high-throughput, high-resolution phenotyping of murine embryos. J Anat 2007; 211: 132-7.

[51] Dhenain M, Ruffins SW, Jacobs RE. Three-dimensional digital mouse atlas using high-resolution MRI. Dev Biol 2001; 232: 458-70.

[52] Turnbull DH, Mori S. MRI in mouse developmental biology. NMR Biomed 2007; 20: 265-74.

[53] Chiverton JP, Wells K. Adaptive partial volume classification of MRI data. Phys Med Biol 2008; 53: 5577-94.

[54] Cohen B, Ziv K, Plaks V, *et al.* MRI detection of transcriptional regulation of gene expression in transgenic mice. Nat Med 2007; 13: 498-503.

[55] Schneider JE, Bhattacharya S. Making the mouse embryo transparent: identifying developmental malformations using magnetic resonance imaging. Birth Defects Res C Embryo Today 2004; 72: 241-9.

[56] Schneider JE, Bose J, Bamforth SD, *et al.* Identification of cardiac malformations in mice lacking Ptdsr using a novel high-throughput magnetic resonance imaging technique. BMC Dev Biol 2004; 4: 16.

[57] Justice MJ, Noveroske JK, Weber JS, Zheng B, Bradley A. Mouse ENU mutagenesis. Hum Mol Genet 1999; 8: 1955-63.

[58] Hrabe de Angelis MH, Flaswinkel H, Fuchs H, *et al.* Genome-wide, large-scale production of mutant mice by ENU mutagenesis. Nat Genet 2000; 25: 444-7.

[59] Justice MJ. Capitalizing on large-scale mouse mutagenesis screens. Nat Rev 2000; 1: 109-15.

[60] Nolan PM, Peters J, Strivens M, *et al.* A systematic, genome-wide, phenotype-driven mutagenesis programme for gene function studies in the mouse. Nat Genet 2000; 25: 440-3.

[61] Nolan PM, Peters J, Vizor L, *et al.* Implementation of a large-scale ENU mutagenesis program: towards increasing the mouse mutant resource. Mamm Genome 2000; 11: 500-6.

[62] Yu Q, Shen Y, Chatterjee B, *et al.* ENU induced mutations causing congenital cardiovascular anomalies. Development 2004; 131: 6211-23.

[63] Cordes SP. N-ethyl-N-nitrosourea mutagenesis: boarding the mouse mutant express. Microbiol Mol Biol Rev 2005; 69: 426-39.

[64] Johnson JT, Hansen MS, Wu I, *et al.* Virtual histology of transgenic mouse embryos for high-throughput phenotyping. PLoS Genet 2006; 2: e61.

[65] Jorgensen SM, Demirkaya O, Ritman EL. Three-dimensional imaging of vasculature and parenchyma in intact rodent organs with X-ray micro-CT. Am J Physiol 1998; 275: H1103-14.

[66] Heinzer S, Krucker T, Stampanoni M, *et al.* Hierarchical micro-imaging for multiscale analysis of large vascular networks. Neuroimage 2006; 32: 626-36.

[67] Butcher JT, Sedmera D, Guldberg RE, Markwald RR. Quantitative volumetric analysis of cardiac morphogenesis assessed through micro-computed tomography. Dev Dyn 2007; 236: 802-9.

[68] Sharpe J, Ahlgren U, Perry P, *et al.* Optical projection tomography as a tool for 3D microscopy and gene expression studies. Science 2002; 296: 541-5.

[69] Sharpe J. Optical projection tomography as a new tool for studying embryo anatomy. J Anat 2003; 202: 175-81.

[70] Breckenridge R, Kotecha S, Towers N, Bennett M, Mohun T. Pan-myocardial expression of Cre recombinase throughout mouse development. Genesis 2007; 45: 135-44.

[71] Bryson-Richardson RJ, Berger S, Schilling TF, *et al.* FishNet: an online database of zebrafish anatomy. BMC Biol 2007; 5: 34.

[72] McGurk L, Morrison H, Keegan LP, Sharpe J, O'Connell MA. Three-dimensional imaging of *Drosophila melanogaster*. PLoS ONE 2007; 2: e834.

[73] Delaurier A, Burton N, Bennet M, *et al.* The mouse limb anatomy atlas: an interactive 3D tool for studying embryonic limb patterning. BMC Biol 2008; 8: 83.

[74] Fisher ME, Clelland AK, Bain A, *et al.* Integrating technologies for comparing 3D gene expression domains in the developing chick limb. Dev Biol 2008; 317: 13-23.

[75] Foolen J, van Donkelaar C, Nowlan N, Murphy P, Huiskes R, Ito K. Collagen orientation in periosteum and perichondrium is aligned with preferential directions of tissue growth. J Orthop Res 2008.

[76] Walls JR, Sled JG, Sharpe J, Henkelman RM. Correction of artefacts in optical projection tomography. BMC Dev Biol 2005; 50: 4645-65.

[77]   Walls JR, Sled JG, Sharpe J, Henkelman RM. Resolution improvement in emission optical projection tomography. BMC Dev Biol 2007; 52: 2775-90.

[78]   DeLaurier A, Schweitzer R, Logan M. Pitx1 determines the morphology of muscle, tendon, and bones of the hindlimb. Dev Biol 2006; 299: 22-34.

[79]   Ijpenberg A, Perez-Pomares JM, Guadix JA, *et al.* Wt1 and retinoic acid signaling are essential for stellate cell development and liver morphogenesis. Dev Biol 2007; 312: 157-70.

[80]   Sato H, Murphy P, Giles S, Bannigan J, Takayasu H, Puri P. Visualizing expression patterns of Shh and Foxf1 genes in the foregut and lung buds by optical projection tomography. Pediatr Surg Int 2008; 24: 3-11.

[81]   Boot MJ, Westerberg CH, Sanz-Ezquerro J, *et al. In vitro* whole-organ imaging: 4D quantification of growing mouse limb buds. Nat Methods 2008; 5: 609-12.

[82]   Ratajska A, Fiejka E. Prenatal development of coronary arteries in the rat: morphologic patterns. Anat Embryol (Berl) 1999; 200: 533-40.

[83]   Webb S, Brown NA, Anderson RH, Richardson MK. Relationship in the chick of the developing pulmonary vein to the embryonic systemic venous sinus. Anat Rec 2000; 259: 67-75.

[84]   Nesbitt TL, Patel PA, Yost MJ, Goodwin RL, Potts JD. A 3-D model of coronary vessel development. *In Vitro* Cell Dev Biol Anim 2007; 43: 10-6.

[85]   Schulte I, Schlueter J, Abu-Issa R, Brand T, Manner J. Morphological and molecular left-right asymmetries in the development of the proepicardium: a comparative analysis on mouse and chick embryos. Dev Dyn 2007; 236: 684-95.

[86]   Weiger T, Lametschwandtner A, Stockmayer P. Technical parameters of plastics (Mercox CL-2B and various methylmethacrylates) used in scanning electron microscopy of vascular corrosion casts. Scan Electron Microsc 1986; (Pt 1): 243-52.

[87]   Lametschwandtner A, Lametschwandtner U, Weiger T. Scanning electron microscopy of vascular corrosion casts--technique and applications: updated review. Scanning Microsc 1990; 4: 889-940.

[88]   Kondo S. Microinjection methods for visualization of the vascular architecture of the mouse embryo for light and scanning electron microscopy. J Electron Microsc 1998; 47: 101-13.

[89]   Djonov VG, Kurz H, Burri PH. Optimality in the developing vascular system: branching remodeling by means of intussusception as an efficient adaptation mechanism. Dev Dyn 2002; 224: 391-402.

[90]   Sangiorgi S, Manelli A, Congiu T, *et al.* Microvascularization of the human digit as studied by corrosion casting. J Anat 2004; 204: 123-31.

[91]   Weninger WJ. Computergestützte dreidimensionale Rekonstruktion histologischer Schnittserien [Dissertation]: Universität Wien; 1995.

[92]   Soufan AT, Ruijter JM, van den Hoff MJ, de Boer PA, Hagoort J, Moorman AF. Three-dimensional reconstruction of gene expression patterns during cardiac development. Physiol Genom 2003; 13: 187-95.

[93]   Soufan AT, van den Hoff MJ, Ruijter JM, *et al.* Reconstruction of the patterns of gene expression in the developing mouse heart reveals an architectural arrangement that facilitates the understanding of atrial malformations and arrhythmias. Circ Res 2004; 95: 1207-15.

[94]   Kaufman MH, Richardson L. 3D reconstruction of the vessels that enter the right atrium of the mouse heart at Theiler Stage 20. Clin Anat 2005; 18: 27-38.

[95]   Mommersteeg MT, Hoogaars WM, Prall OW, *et al.* Molecular pathway for the localized formation of the sinoatrial node. Circ Res 2007; 100: 354-62.

[96]   Soufan AT, van den Berg G, Moerland PD, *et al.* Three-dimensional measurement and visualization of morphogenesis applied to cardiac embryology. J Microsc 2007; 225: 269-74.

[97]   Weninger WJ, Streicher J, Müller GB. [3-dimensional reconstruction of histological serial sections using a computer]. Wien Klin Wochenschr 1996; 108: 515-20.

[98]   Streicher J, Weninger WJ, Müller GB. External marker-based automatic congruencing: a new method of 3D reconstruction from serial sections. Anat Rec 1997; 248: 583-602.

[99]   Streicher J, Müller GB. 3D modelling of gene expression patterns. Trends Biotechnol 2001; 19: 145-8.

[100]  Soufan AT, van den Berg G, Ruijter JM, de Boer PA, van den Hoff MJ, Moorman AF. Regionalized sequence of myocardial cell growth and proliferation characterizes early chamber formation. Circ Res 2006; 99: 545-52.

[101]  Kolker SJ, Tajchman U, Weeks DL. Confocal imaging of early heart development in *Xenopus laevis*. Dev Biol 2000; 218: 64-73.

[102]  Lawson ND, Weinstein BM. *In vivo* imaging of embryonic vascular development using transgenic zebrafish. Dev Biol 2002; 248: 307-18.

[103]  Liebling M, Forouhar AS, Gharib M, Fraser SE, Dickinson ME. Four-dimensional cardiac imaging in living embryos *via* postacquisition synchronization of nongated slice sequences. J Biomed Opt 2005; 10: 054001.

[104]  Landmann L. Deconvolution improves colocalization analysis of multiple fluorochromes in 3D confocal data sets more than filtering techniques. J Microsc 2002; 208: 134-47.

[105]  Difato F, Mazzone F, Scaglione S, *et al.* Improvement in volume estimation from confocal sections after image deconvolution. Microsc Res Tech 2004; 64: 151-5.

[106]  Hecksher-Sorensen J, Sharpe J. 3D confocal reconstruction of gene expression in mouse. Mech Dev 2001; 100: 59-63.

[107]  Ahnfelt-Ronne J, Jorgensen MC, Hald J, Madsen OD, Serup P, Hecksher-Sorensen J. An improved method for three-dimensional reconstruction of protein expression patterns in intact mouse and chicken embryos and organs. J Histochem Cytochem 2007; 55: 925-30.

[108]  Odgaard A, Andersen K, Melsen F, Gundersen HJ. A direct method for fast three-dimensional serial reconstruction. J Microsc 1990; 159: 335-42.

[109]  Weninger WJ, Meng S, Streicher J, Müller GB. A new episcopic method for rapid 3-D reconstruction: applications in anatomy and embryology. Anat Embryol (Berl) 1998; 197: 341-8.

[110]  Ewald AJ, McBride H, Reddington M, Fraser SE, Kerschmann R. Surface imaging microscopy, an automated method for visualizing whole embryo samples in three dimensions at high resolution. Dev Dyn 2002; 225: 369-75.

[111]  Weninger WJ, Geyer SH, Mohun TJ, *et al.* High-resolution episcopic microscopy: a rapid technique for high detailed 3D analysis of gene activity in the context of tissue architecture and morphology. Anat Embryol 2006; 211: 213-21.

[112]  Gerneke DA, Sands GB, Ganesalingam R, *et al.* Surface imaging microscopy using an ultramiller for large volume 3D reconstruction of wax- and resin-embedded tissues. Microsc Res Tech 2007; 70: 886-94.

[113]  Weninger WJ, Geyer SH. Episcopic 3D imaging methods: tools for researching gene function. Curr Genomics 2008; 9: 282-9.

[114]  Weninger WJ, Mohun TJ. Three-dimensional analysis of molecular signals with episcopic imaging techniques. Methods Mol Biol 2007; 411: 35-46.